

Elastic Transfer: A Nondispersive Component in the Optical Potential, and its Effect on the $^{12}\text{C} + ^{24}\text{Mg}$ Elastic Scattering

A. Lépine-Szily,¹ M. S. Hussein,¹ R. Lichtenthäler,¹ J. Cseh,² and G. Lévai²

¹*IFUSP-Universidade de São Paulo, C.P. 66318, 5315-970 São Paulo, Brasil*

²*MTA ATOMKI, Debrecen Pf.51, Hungary-4001*

(Received 9 November 1998)

It is emphasized that the coupling of the elastic channel to an elastic transfer channel leads to a nondispersive polarization potential with a periodic energy dependence. Evidence of this is found in the elastic scattering data of $^{12}\text{C} + ^{24}\text{Mg}$ at low energies. The finding hints at a significant $^{12}\text{C} + ^{12}\text{C}$ clustering effect in the ground state of ^{24}Mg . [S0031-9007(99)09159-0]

PACS numbers: 24.10.Ht, 25.70.Bc, 27.30.+t

Clustering in many-fermion systems is a very intriguing phenomenon. A well-known example of this is the pairing effect in superconductors and in nuclei. Here bosonlike entities become effective degrees of freedom in the otherwise Fermi environment. Heavier clusters, such as α particles in nuclei, are also known to be important degrees of freedom. Usually, well-formed cluster states in nuclei are found above the ground state, such as the famous Hoyle 3 α resonance in ^{12}C and the quasilinear 6 α chain in ^{24}Mg . It is certainly very interesting to assess whether there is a hierarchy of clustering: α , ^{12}C , etc. As is already well known, ^{24}Mg contains an important component in several of its excited state wave functions, which corresponds to two ^{12}C clusters. How much of the ^{12}C clustering is there in the ground state of such a nucleus?

The purpose of this Letter is to supply evidence of such a ground state clustering effect. We show this by providing an analysis of the elastic scattering angular distributions at low bombarding energies of the systems $^{12}\text{C} + ^{24}\text{Mg}$ and $^{12}\text{C} + ^{28}\text{Si}$. The importance of the elastic transfer, a manifestation of such clustering is clearly demonstrated for the former system. The basis of our analysis is the nondispersive nature of the elastic transfer polarization potential, which we describe below.

The dispersive optical potential usually referred to as the Feshbach potential [1], obeys a dispersion relation. In the heavy ion context this relation has gained notoriety in recent years and is usually referred to as the threshold anomaly. As eloquently explained by Satchler [2], the dispersion relation of the Feshbach potential comes about as a consequence of the polarization nature in the sense that the potential has the general structure

$$V_F(r, r') = \sum_{i=1}^n V_{0i}(r) \langle r | \frac{1}{E - H_i + i\epsilon} | r' \rangle V_{i0}(r'). \quad (1)$$

The intermediate channel Green operator, $(E - H_i + i\epsilon)^{-1}$, has the simple structure

$$(E - H_i + i\epsilon)^{-1} = -i\pi\delta(E - H_i) + P \frac{1}{E - H_i}, \quad (2)$$

where P stands for the principal part and H_i is taken for simplicity to be Hermitian. Clearly, one can write

$$P \frac{1}{E - H_i} = P \int dz \frac{\delta(z - H_i)}{E - z} = -\frac{P}{\pi} \int dz \frac{-\pi\delta(z - H_i)}{E - z}. \quad (3)$$

From Eqs. (1) and (3), one finds the dispersion relation

$$\text{Re}V_F(r, r', E) = \frac{P}{\pi} \int dz \frac{\text{Im}V_F(z, r, r')}{z - E}, \quad (4)$$

which can be generalized to the whole V_F [Eq. (1)]. The generalization of the dispersion relation for the case of non-Hermitian H_i is given in Ref. [3]. This reference shows that Eq. (4) still holds. In actual use in data analysis one relies on local potentials. The intrinsically nonlocal dispersive Feshbach potential is therefore transformed into a local-equivalent one. This brings in more subtle energy dependence. We should point out that the nondispersive “bare” part of the interaction is also nonlocal owing to the Pauli exchange effects. In its local-equivalent version the bare interaction also carries important energy dependence as has been stressed recently in [4–6]. In practical application, it was found [7] that the local-equivalent Feshbach potential, at a given value of the now one spatial variable r , still satisfies Eq. (4).

We now raise the following question: Do all channel couplings result in a dispersive Feshbach potential? The answer is “no,” at least in cases involving elastic transfer. Here we mean a process which involves the elastic scattering of the following objects:

$$(a + b) + b \rightarrow (a + b) + b, \quad (5)$$

$$(a + b) + b \rightarrow b + (a + b). \quad (6)$$

The two corresponding amplitudes add coherently. Since the projectile-target system, in the second process, becomes the target-projectile system (no change in internal structure), the second process in Eq. (6), the elastic transfer process, is important at large angles. The Feshbach

potential that takes into account the coupling of the elastic channel to the elastic transfer channel is found to be [8,9]

$$V_F^{\text{elastic transfer}} = (-1)^l F(r), \quad (7)$$

where l is the orbital angular momentum and $F(r)$ is an approximate transfer form factor of the second process in Eq. (6). Generally, owing to the strong nonlocal character of the exchange process, the form factor $F(r)$ should be taken to be the local equivalent version of the otherwise nonlocal form factor. This implies a *nondispersive* energy dependence in $V_F^{\text{elastic transfer}}$ quite distinct from the genuine dispersive Feshbach potential. There is no dispersive energy dependence in (7). Clearly, (7) does not satisfy any energy dispersion relation. Of course some weak energy dependence may be found in $V_F^{\text{elastic transfer}}$, when higher-order processes are taken into account, e.g.,

$$(a + b) + b \rightarrow (a + b)^* + b \rightarrow b + (a + b). \quad (8)$$

For simplicity, in the following we ignore these processes.

In a recent experiment [10,11] the complete angular distributions of the elastic scattering of $^{12}\text{C} + ^{24}\text{Mg}$ were measured at fifteen energies near the Coulomb barrier, namely, between $E_{c.m.} = 10.67$ and 16.00 MeV. The data were analyzed in the optical model framework (Pot.II) and the best-fit potentials were shallow, energy dependent, real potentials ($V_0 \sim 37$ MeV, $r_0 = 1.29$ fm, $a = 0.4$ fm) with no continuous ambiguity and very weak, energy dependent, imaginary potentials ($W_0/V_0 \sim 0.01$, $W_0 = 0.5-1.5$ MeV, $r_i = 1.77$ fm, $a_i \sim 0.4-0.8$ fm).

We present in Fig. 1a some of the lowest energy angular distributions, situated at energies under and at the Coulomb barrier ($V_{CB} = 12.67$ MeV using the Christensen-Winther radius) together with the optical model fits. The angular distributions present a clear oscillatory pattern even at the lowest energies. In Fig. 1b the low-energy elastic scattering angular distributions of the $^{12}\text{C} + ^{28}\text{Si}$ system are presented. These unpublished data [12] were also measured at the Pelletron Laboratory of the São Paulo University, and will be published in the near future together with an optical model analysis. The optical model used to reproduce the data is much more absorptive (3 to 5 times more) than the Pot.II used for the $^{12}\text{C} + ^{24}\text{Mg}$ system. The Christensen-Winther Coulomb barrier for the $^{12}\text{C} + ^{28}\text{Si}$ system is $V_{CB} = 14.36$ MeV. We indicate in the figure caption the ratio $E_{c.m.}/V_{CB}$ to allow a quantitative comparison between angular distributions of Figs. 1a and 1b.

While the oscillations are clear for the $^{12}\text{C} + ^{24}\text{Mg}$ system, even at energies under the Coulomb barrier, they are smooth and nonoscillating for the $^{12}\text{C} + ^{28}\text{Si}$ system at the same energies. Even at energies 12% above the Coulomb barrier, where the very back angle region of the $^{12}\text{C} + ^{28}\text{Si}$ begins to show one oscillation, the $^{12}\text{C} + ^{24}\text{Mg}$ system shows much more oscillation in the intermediate angle region.

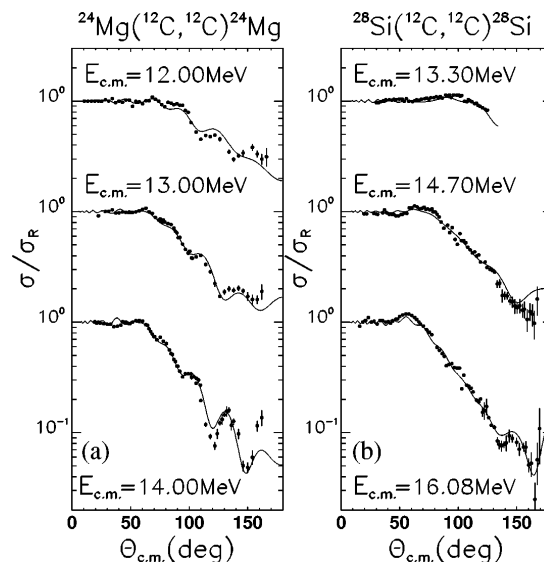


FIG. 1. (a) The $^{12}\text{C} + ^{24}\text{Mg}$ elastic scattering angular distributions, measured at the indicated energies, are represented by the dots. The solid lines are optical model calculations with our best-fit optical potentials (Pot.II). The $E_{c.m.}/V_{CB}$ values at these energies are respectively, 0.947, 1.026, and 1.105, with $V_{CB} = 12.67$ MeV. (b) The $^{12}\text{C} + ^{28}\text{Si}$ elastic scattering angular distributions, measured at the indicated energies, are represented by the dots. The $E_{c.m.}/V_{CB}$ values at these energies are, respectively, 0.926, 1.023, and 1.120 with $V_{CB} = 14.36$ MeV.

Both optical potentials are dependent on the bombarding energy. From the point of view of radial dependences, their differences can be pinned down in the notch test [11]. It showed very different results for the two systems. For the $^{12}\text{C} + ^{28}\text{Si}$ system the notch test presents a localized peak at $R_1 + R_2 = 7.3$ fm, which means that the elastic data are sensitive to the optical potential only in a radially restricted region at the nuclear surface at about 7.3 fm. For the $^{12}\text{C} + ^{24}\text{Mg}$ system the notch test indicates that the elastic data are sensitive to the optical potential on the surface and in the nuclear interior, from 3 to 8 fm, results compatible with the very transparent optical potentials used to fit the data [11].

Such optical potentials will introduce reflections in the effective potentials which would dominate the internal wave contribution and whose interference with the external wave would result in the oscillations seen in the cross sections [13]. The internal wave contribution seems, however, completely damped in the $^{12}\text{C} + ^{28}\text{Si}$ system. What causes the great qualitative difference between the potentials of the two systems may be related to the fact that ^{24}Mg and ^{28}Si have quite different cluster properties.

The differences between the two potentials become even more interesting when they are compared from the point of view of their energy dependences, through the dispersion relation [Eq. (4)]. While the optical potentials of the $^{12}\text{C} + ^{28}\text{Si}$ system satisfy the dispersion relation at the $R = 7.3$ fm, the optical potentials of the $^{12}\text{C} + ^{24}\text{Mg}$

system do not satisfy the dispersion relation at any radius (see Fig. 2). Nevertheless, the volume integrals of the optical potentials of the $^{12}\text{C} + ^{24}\text{Mg}$ system satisfy the dispersion relation as shown previously [10,11].

The difference between the real part of the fit optical potential and the real potential obtained through the dispersion relation using the fit imaginary part is plotted in Fig. 3. In the case of the $^{12}\text{C} + ^{28}\text{Si}$ system, at least at these very low energies, the difference $\text{Re}V_{\text{nondispersive}}$ is zero, while for the $^{12}\text{C} + ^{24}\text{Mg}$ system it presents a clearly oscillatory pattern, as a function of energy and with a decreasing amplitude, when the radius increases. If we assume that the nondispersive part of the potential is responsible for the coupling of the elastic channel to the elastic transfer channel, then, from the point of view of Eqs. (4) and (7), we can write

$$\begin{aligned} \text{Re}V_{\text{opt mod}} - \text{Re}V_{\text{F}} &= \text{Re}V_{\text{nondispersive}} \\ &= (-1)^l F(r) \\ &= \cos(\pi l(r, E)) F(r), \end{aligned} \quad (9)$$

where a semiclassical interpretation was invoked to transform the l dependence into r and E dependences. Here, $l(r, E)$ is a function to be obtained from the classical turning point condition

$$E = V(r) + \frac{\hbar^2 l(l+1)}{2\mu r^2}. \quad (10)$$

Then, qualitatively, the nondispersive part of the potential should have an oscillatory character ($\cos \pi l$) and decrease in amplitude with increasing r [$F(r)$], as it appears in

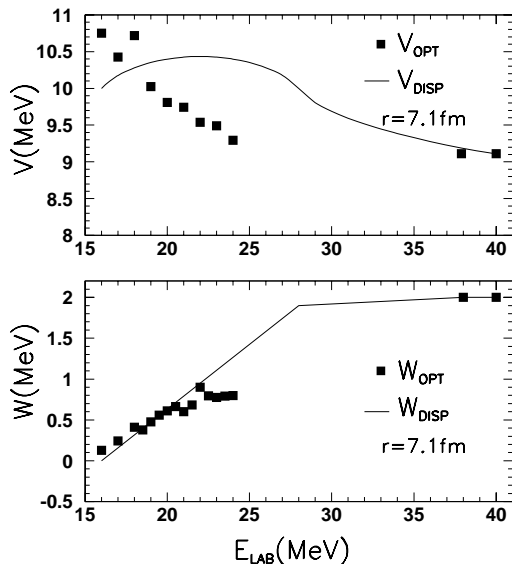


FIG. 2. The imaginary and the real depths of the best-fit optical potentials of the $^{12}\text{C} + ^{24}\text{Mg}$ system, as a function of the laboratory energies (squares) for $R = 7.1$ fm. We also used data at higher energies ($E_{\text{lab}} = 37.9$ and 40.0 MeV [10,11]) to fix the imaginary part of the potential. The dispersion relation calculations are indicated by solid lines and the disagreement with the real optical potential is evident.

Fig. 3. We also show in Fig. 3 a very qualitative fit to $\text{Re}V_{\text{nondispersive}}$ by a cosine function. We assumed that the argument of the cosine function, which is $\pi \tilde{l}$, where \tilde{l} is an orbital angular momentumlike quantity, varies as \sqrt{E} and linearly with r . The argument for the cosine function in the three fits was roughly

$$\pi \tilde{l} = \text{const} \times \sqrt{E} r. \quad (11)$$

This is different from that obtained from the classical turning point relation $\tilde{l} = \text{const} \sqrt{1 - V/E} \sqrt{E} r$.

Note that the volume integral of the right-hand side of Eq. (9) is roughly zero, in accordance with our earlier discussion.

The reaction amplitudes of Eqs. (5) and (6) can interfere only in case the cluster b is present in the target. Thus, from the nuclear structure point of view the crucial question is whether or not the (exotic) cluster corresponding to the projectile nucleus is present in the ground state of the target. The phenomenon of clustering in light nuclei has received considerable attention in the literature [14].

For different samples of light nuclei selection rules obtained from U(3) symmetry [15,16] have been applied systematically [17]. As a result we have found that (in the leading term approximation) the ^{12}C cluster is present in the ground state of the ^{24}Mg nucleus, but is absent from the ground state of the ^{28}Si . (For these two nuclei more detailed cluster calculations have also been carried out in the algebraic framework, which incorporated a large number of excited states as well [18].)

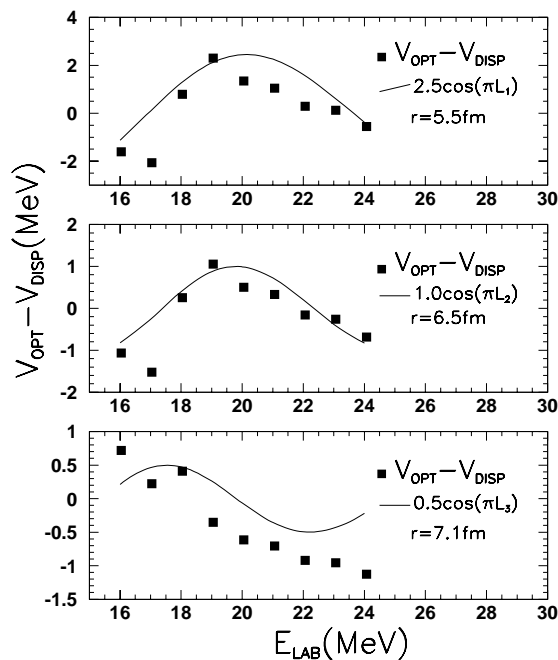


FIG. 3. The difference between the real part of the optical potential and the real part of the dispersive potential (calculated by the dispersion relation) as a function of the laboratory energy, at three radial positions, $R = 5.5, 6.5,$ and 7.1 . See text for discussion of the solid line.

The different oscillatory pattern of Figs. 1a and 1b, as well as the different nature of the corresponding potentials, as discussed previously, seems to justify the predictions of the nuclear cluster model. Actually, the coherence effect between the reaction amplitudes of Eqs. (5) and (6) can be considered as the fingerprint of the exotic (projectilelike) clusterization in the ground state of the target nucleus.

Before concluding, we raise a second question: Namely, since the light nuclei considered here are known to exhibit significant α clustering, what would be the relevance of α -transfer couplings to our conclusions? This question has been extensively discussed and answered in an earlier publication [11]. To begin with, the absence of oscillations in the $^{12}\text{C} + ^{28}\text{Si}$ system already indicates that this effect is strongly damped at these energies. Accordingly, the corresponding dispersive polarization potentials are expected to be unimportant. The situation changes at higher energies [19,20], where these polarization potentials become narrower in l space and stronger in intensity, thus affecting the back-angle elastic angular distributions more. Although at energies significantly higher than ours, both $^{12}\text{C} + ^{24}\text{Mg}$ and $^{12}\text{C} + ^{28}\text{Si}$ show marked "quasimolecular" structures in the elastic excitation functions, no such feature is seen at the low energies considered here [11,21].

In conclusion, we have shown that the fits to the $^{12}\text{C} + ^{24}\text{Mg}$ elastic scattering data with a shallow potential produce conspicuous oscillatory structures in the angular distributions, which we attribute to the coupling to the elastic transfer channel. The energy dependence of our best-fit real shallow potential is identified with nondispersive parity-dependent polarization effects. Thus, clear experimental evidence has been presented in this paper in favor of a nondispersive component in the Feshbach potential, which is traced to the coupling of the elastic channel to an elastic transfer channel. This finding may shed light on the cluster effect in the ground state of light nuclei. Further, the findings in this paper may prove of great value in reactions induced by halo nuclei, where clustering of the type core + halo is important. Applications to the elastic transfer process in the $^{11}\text{Be} + ^{10}\text{Be}$ at low energies is in progress [22].

The first three authors are partially supported by CNPq and FAPESP and the last two by OTKA (Grant No. T22187).

[1] H. Feshbach, *Theoretical Nuclear Physics II, Nuclear Reactions* (Wiley, New York, 1992).

- [2] G. R. Satchler, *Phys. Rep.* **199**, 147 (1991).
 [3] B. V. Carlson, T. Frederico, M. S. Hussein, H. Esbensen, and S. Landowne, *Phys. Rev. C* **41**, 933 (1990).
 [4] M. A. Cândido Ribeiro, L. C. Chamon, D. Pereira, M. S. Hussein, and D. Galetti, *Phys. Rev. Lett.* **78**, 3270 (1997).
 [5] L. C. Chamon, D. Pereira, M. S. Hussein, M. A. Cândido Ribeiro, and D. Galetti, *Phys. Rev. Lett.* **79**, 5218 (1997).
 [6] L. C. Chamon, D. Pereria, and M. S. Hussein, *Phys. Rev. C* **58**, 576 (1998).
 [7] C. Mahaux, H. Ngô, and G. R. Satchler, *Nucl. Phys.* **A449**, 354 (1986).
 [8] W. E. Frahn, *Diffraction Processes in Nuclear Physics* (Clarendon Press, Oxford, 1985).
 [9] W. von Oertzen and H. G. Bohlen, *Phys. Rep.* **19**, 1 (1975).
 [10] A. Lépine-Szily, W. Sciani, Y. K. Watari, W. Mittig, R. Lichtenthäler, M. M. Obuti, J. M. Oliveira, Jr., and A. C. C. Villari, *Phys. Lett. B* **304**, 45 (1993).
 [11] W. Sciani, A. Lépine-Szily, R. Lichtenthäler, P. Fachini, L. C. Gomes, G. F. Lima, M. M. Obuti, J. M. Oliveira, Jr., and A. C. C. Villari, *Nucl. Phys.* **A620**, 91 (1997).
 [12] J. M. Oliveira, Jr., M.Sc. thesis, IFUSP (unpublished).
 [13] D. M. Brink and N. Takigawa, *Nucl. Phys.* **A279**, 159 (1977).
 [14] For a review on clustering in light nuclei, see, e.g., B. R. Fulton and W. D. Rae, *J. Phys. G* **16**, 333 (1990); M. Freer and A. C. Merchant, *J. Phys. G* **23**, 261 (1997), and reference therein.
 [15] J. P. Elliott, *Proc. R. Soc. London A* **245**, 128 (1958); **245**, 562 (1958).
 [16] K. Wildermuth and Th. Kanellopoulos, *Nucl. Phys.* **7**, 150 (1958); K. Wildermuth and Y. C. Tang, *A Unified Theory of the Nucleus* (Academic, New York, 1977).
 [17] J. Cseh and W. Scheid, *J. Phys. G* **18**, 1419 (1992); J. Cseh, *J. Phys. G* **19**, L97 (1993).
 [18] J. Cseh, G. Lévai, and W. Scheid, *Phys. Rev. C* **48**, 1724 (1993); J. Cseh, *Phys. Rev. C* **50**, 2240 (1994).
 [19] A. Lépine-Szily, M. M. Obuti, R. Lichtenthäler, J. M. Oliveira, Jr., and A. C. C. Villari, *Phys. Lett. B* **243**, 23 (1990); R. Lichtenthäler, A. Lépine-Szily, A. C. C. Villari, W. Mittig, V. J. G. Porto, and C. V. Acquadro, *Phys. Rev. C* **26**, 2487 (1982).
 [20] R. Lichtenthäler, A. Lépine-Szily, A. C. C. Villari, and O. Portezan, *Phys. Rev. C* **39**, 884 (1989); A. Lépine-Szily, R. Lichtenthäler, O. Portezan, J. M. Oliveira, Jr., M. M. Obuti, and A. C. C. Villari, *Phys. Rev. C* **40**, 681 (1989).
 [21] R. R. Betts and A. H. Wuosmaa, *Rep. Prog. Phys.* **60**, 819 (1997).
 [22] R. Lichtenthäler, A. Lépine-Szily, and M. S. Hussein (to be published).